

Nicotine and Cotinine Exposure from Electronic Cigarettes: A Population Approach

Nieves Vélez de Mendizábal · David R. Jones ·
Andy Jahn · Robert R. Bies · Joshua W. Brown

Published online: 12 December 2014
© Springer International Publishing Switzerland 2014

Abstract

Background and Objectives Electronic cigarettes (e-cigarettes) are a recent technology that has gained rapid acceptance. Still, little is known about them in terms of safety and effectiveness. A basic question is how effectively they deliver nicotine; however, the literature is surprisingly unclear on this point. Here, a population pharmacokinetic model was developed for nicotine and its major metabolite cotinine with the aim to provide a reliable framework for the simulation of nicotine and cotinine concentrations over time, based solely on inhalation airflow recordings and individual covariates [i.e., weight and breath carbon monoxide (CO) levels].

Methods This study included ten adults self-identified as heavy smokers (at least one pack of cigarettes per day). Plasma nicotine and cotinine concentrations were measured at regular 10-min intervals for 90 min while human subjects inhaled nicotine vapor from a modified e-cigarette. Airflow measurements were recorded every 200 ms throughout the session. A population pharmacokinetic model for nicotine

and cotinine was developed based on previously published pharmacokinetic parameters and the airflow recordings. All of the analyses were performed with the non-linear mixed-effect modeling software NONMEM[®] version 7.2.

Results The results show that e-cigarettes deliver nicotine effectively, although the pharmacokinetic profiles are lower than those achieved with regular cigarettes. Our pharmacokinetic model effectively predicts plasma nicotine and cotinine concentrations from the inhalation volume, and initial breath CO.

Conclusion E-cigarettes are effective at delivering nicotine. This new pharmacokinetic model of e-cigarette usage might be used for pharmacodynamic analysis where the pharmacokinetic profiles are not available.

Electronic supplementary material The online version of this article (doi:10.1007/s40262-014-0221-7) contains supplementary material, which is available to authorized users.

N. Vélez de Mendizábal (✉) · R. R. Bies
Division of Clinical Pharmacology, Department of Medicine,
Indiana University School of Medicine, West Walnut Street,
Indianapolis, IN 46202, USA
e-mail: nvelezde@iu.edu

N. Vélez de Mendizábal · D. R. Jones · R. R. Bies
Indiana Clinical and Translational Sciences Institute (CTSI),
Indianapolis, IN, USA

A. Jahn · J. W. Brown
Department of Psychological and Brain Sciences, Indiana
University, Bloomington, IN 47405, USA

Key Points

Electronic cigarettes (e-cigarettes) are rapidly gaining acceptance, but their pharmacokinetic effect with respect to nicotine is unclear.

We measured initial carbon monoxide breath, e-cigarette inhalation airflow, and plasma nicotine and cotinine concentrations for 90 min while human subjects were using the e-cigarette. Based on these data we developed a population pharmacokinetic model able to simultaneously describe nicotine and cotinine profiles in plasma.

E-cigarettes deliver nicotine effectively, although the pharmacokinetic profiles are lower than those achieved with regular cigarettes. The model might be extremely useful for nicotine drug–effect analysis and quantification when the actual pharmacokinetic profiles are not available.

1 Introduction

The pharmacokinetics of nicotine and cotinine are well-characterized in humans [1–3]. In 1992, Robinson et al. [1–3] published a reliable physiologically based pharmacokinetic (PBPK) model describing the disposition kinetics of nicotine and its major metabolite cotinine in humans. Very recently, Teeguarden et al. [2] published a multi-route model of nicotine–cotinine pharmacokinetics, also in humans. They also developed a PBPK model of nicotine and cotinine in humans after administration via intravenous, oral, and inhalation routes using cigarettes (nicotine yield 1.3 mg). Since the most common administration route for nicotine is inhalation, a focus on intravenous and oral administration route pharmacokinetics analysis might be limited.

The use of electronic cigarettes (e-cigarettes) has increased dramatically over the past few years, leading to a host of legal and regulatory issues over how to classify e-cigarettes. An e-cigarette is a battery-powered device that simulates tobacco smoking. These e-cigarettes generally use a small heating element that vaporizes a liquid solution containing the active ingredients, water, and propylene glycol or a similar solvent. The user simply inhales the resulting vapor in a process called ‘vaping’, an action similar to regular smoking but with electronic cigarette vapor. Some solutions contain a mixture of nicotine and flavorings, while others release a flavored vapor without nicotine. E-cigarette users generally perceive e-cigarettes to be effective at reducing nicotine cravings and also perceive them to be less harmful than regular cigarettes [4, 5]. The benefits and risks of e-cigarette use are uncertain as the technology is relatively new. While e-cigarettes may be less harmful than regular cigarettes, they may still contain impurities and toxic ingredients [6]. There is some evidence that they are effective at delivering nicotine [7–9], as e-cigarettes lead to similar plasma cotinine elevations as regular cigarettes [10], although they may yield less nicotine per puff [11]. Users may need a period of weeks to learn how to use them to deliver the most nicotine. Individuals new to e-cigarettes typically obtain lower plasma nicotine concentrations initially, but after 4 weeks of experience with e-cigarettes they are able to achieve higher plasma nicotine concentrations and significantly greater overall nicotine intake [12]. However, the literature is ambiguous on how effectively e-cigarettes deliver nicotine to users, as some have reported no measurable increases in plasma nicotine following e-cigarette usage [13, 14]. The current study addresses how effectively e-cigarettes may deliver nicotine, and how well the delivery can be described with a pharmacokinetic model.

For the current study, a customized e-cigarette was developed to allow precise measurements of the heated air temperature and time course of inhaled nicotine vapor volume. This allowed for precise control of and measurement of the nicotine vapor delivered. The developed e-cigarette device is also compatible with magnetic resonance imaging (MRI) to allow direct functional neuroimaging during electronic cigarette usage in future studies. This allows for direct measurement of brain activity while subjects make decisions about using nicotine as an addictive drug. First, however, it is necessary to characterize the nicotine delivery resulting from inhalation from e-cigarettes and the custom device described in this paper specifically. It should be noted that this custom e-cigarette was designed to be MRI-compatible, and although it provides the same functionality as open-market e-cigarettes, we did not explicitly compare its performance with available e-cigarettes (see Sect. 4.4).

In this work, a population pharmacokinetic model for nicotine and its major metabolite cotinine was developed, based on the airflow recordings of e-cigarettes, the loading dose (L_D) for the e-cigarette, the individual covariates, and on the nicotine and cotinine pharmacokinetic parameters published by Robinson et al. [3]. The purpose of this model was to provide a framework for the simulation of nicotine and cotinine concentrations over time, based solely on airflow recordings and individual covariates (i.e., weight and initial CO levels). To the best of our knowledge, this is the first population pharmacokinetic model describing nicotine and cotinine exposure with the use of e-cigarettes. This model can be used for pharmacodynamic analysis where the pharmacokinetic profiles are not available.

2 Methods

2.1 Electronic Nicotine Delivery System: Custom e-Cigarette

A customized electronic nicotine delivery system, ‘custom e-cigarette’, compatible with MRI was developed. The custom e-cigarette is contained in an approximately 12-inch long section of 2-inch diameter PVC tubing. Inside the tubing is a ceramic heater set to maintain a controlled temperature of 300 °F. The heated air is drawn over a small wad of non-ferromagnetic metallic wool, which serves to provide a matrix with a large surface area for the heated air to vaporize the nicotine liquid. The wool is also non-combustible at the temperatures used, which helps avoid a burnt smell that otherwise may occur in e-cigarettes. The wool was loaded with 0.45 mL of 18 mg/mL nicotine liquid (JC Original™ Smoke Juice; Johnson Creek Enterprises, LLC, Johnson Creek, WI, USA; ISO 9001:2008

certified). We chose a US-based smoke juice supplier to minimize concerns regarding the quality and purity of the smoke juice, and we used an external supplier so that we could provide a realistic e-cigarette experience. Nicotine is readily absorbed in liquid form through the skin, so the custom e-cigarette was never loaded with more than 0.45 mL at a time in order to minimize the risk of nicotine overdose from accidental liquid contact or ingestion. The heated air vaporizes the liquid held in the metal wool, and the heated nicotine vapor then flows into a 12-inch long, 0.5-inch diameter clear plastic tube. At the other end of the tube there is a disposable one-way valve that is inserted into the subject's mouth. In this way subjects can inhale heated nicotine vapor. The exhaled breath is subsequently vacuumed from a facemask on the subject's face and then forced through a carbon filter to avoid filling the experiment room with nicotine vapor.

The air flow into the custom e-cigarette is measured and controlled by a Controller. The Controller maintained the ceramic heater at 300 °F and included an air flow measuring device (Omega FMA1700/1800; Omega, Stamford, CT, USA). Air flow measurements were sampled at 5 Hz by an A-to-D converter and stored in a host computer for further processing. The Controller also had a solenoid valve that allowed access to the custom e-cigarette to be enabled or disabled by a host computer, but this feature was not used in the current study as the device was kept open for ad libitum consumption.

2.2 Study Design

Subjects were included in the study if they self-identified as heavy smokers (at least one pack of cigarettes per day) and had no stated intention of trying to stop smoking. Subjects ($N = 10$, five females, ages 18–24 years, mean 20.3 years) gave informed consent to participate. All procedures were reviewed and approved by the Indiana University Institutional Review Board. Subjects were asked to abstain from smoking for 6 h prior to the study. After providing informed consent, the subjects were then weighed. Their exhaled breath carbon monoxide (CO) was measured (Smokerlyzer[®] piCO[™]; Covita, Haddonfield, NJ, USA) in parts per million. This measurement provided some information about how recently the subjects had likely smoked and how much. More importantly, it also allowed us the option to screen out subjects who had recently smoked substantially and were therefore not likely to desire significant additional nicotine at the time [15]. The fact that subjects knew we would perform an initial CO screen provided additional incentive for them to abstain from cigarettes prior to the session. In practice, no subjects were excluded for excessive exhaled CO. After the CO measurement, study subjects were seated comfortably and then

given an intravenous saline lock cannula by a registered nurse. The nurse drew 4 mL of blood at the start of the experiment and then again every 10 min throughout the experiment, for a total of ten blood draws throughout the 90 min session. Subjects were instructed to sit comfortably and inhale ad libitum for the duration. In some cases, if subjects noted that the vapor seemed to be depleted of nicotine, an additional amount of nicotine liquid was added to the custom e-cigarette. After the procedure, the blood samples were spun down for 10 min, and the plasma was pipetted off and stored at -20 °C. Four additional subjects completed the study but could not be analyzed due to equipment malfunction, leaving ten subjects reported in the analyses below.

2.3 Mass Spectroscopy Analysis

Nicotine, (\pm) cotinine, trans-3'-OH cotinine, and (S)cotinine *N*-oxide were quantified in plasma using phenacetin as the internal standard, liquid-liquid extraction, and high-performance liquid chromatography (HPLC)-tandem mass spectrometry (HPLC-MS/MS) (API3200[™]; Applied Biosystems, Foster City, CA, USA). Separation of all analytes was performed with gradient HPLC (acetonitrile: 10 mmol/L ammonium acetate, pH = 5.0) using a CN column [Luna[®] (Phenomenex, Torrance, CA, USA), 5 μ m, 4.6 \times 150 mm]. The mass spectrometer was run in positive mode and the Q1/Q3 settings for each analyte were 163/130, 177/80, 193/80, 193/96, and 180/65 for nicotine, cotinine, trans-3'-OH cotinine, cotinine-*N*-oxide, and phenacetin, respectively. In total, 560 concentrations were measured (140 \times 4 analytes). The limit of quantification (LOQ) is 0.1 ng/mL for both compounds: 32 measurements were below the LOQ (BLQ) (5.71 %).

2.4 Data Analysis

All analyses were performed using NONMEM[®] version 7.2 (Icon Development Solutions, Hanover, MD, USA). BLQ data were reported for both nicotine and metabolite at 0.1 ng/mL (see Sect. 2.3 for more details). BLQ values were included in the analyses and treated as censored information using the M3 method [18]. With the M3 method, the BLQ observations in particular are taken to be the likelihoods that these observations are indeed below the limit. The Laplacian numerical estimation method was used for parameter estimation. Nicotine and cotinine concentrations were simultaneously described. Due to the specific study design, some of the pharmacokinetic parameters were fixed to literature values. Inter-subject variability (ISV) was modeled using exponential functions. An additive model was used to describe residual variability for log-transformed data. This is consistent with a

proportional error on the linear scale. Other residual error structures were also evaluated (e.g., combined error).

2.4.1 Dose and Airflow

Inhaled nicotine is assumed to enter lung blood instantaneously, consistent with experimental data showing rapid uptake via inhalation [16, 17]. The amount of nicotine that reaches the systemic circulation is assumed to be proportional to the airflow recordings. The inhaled airflow was recorded every 200 milliseconds throughout the 90 min session, even when the subject was not actively inhaling. Therefore, the airflow recordings were processed as follows: (1) every negative value was transformed to zero; (2) the 97.5th percentile of the airflow values was calculated based on all subjects (0.4 mL/min); and (3) every value below this threshold was transformed to zero, implying no drug input at those times. The selection of the 97.5th percentile was based on the empirical distribution function of the airflows (no negative values) (see Electronic Supplementary Material, Online Resource 1) with the aim to ensure the identification of the dose events (the patient is inhaling nicotine vapor) and to reduce the noise in the inputs. The dose events were defined based on this processed airflow (airflow_P), the custom e-cigarette L_D (18 mg/mL), and a scaling factor (F), as in Eq. 1:

$$\text{dose} = \text{airflow}_P \times L_D \times F \quad (1)$$

The parameter F is a scaling factor that links the airflow recoding and the L_D with the actual drug amount that reaches the systemic circulation.

2.4.2 Pharmacokinetic Modeling

The population pharmacokinetic model for nicotine and its major metabolite cotinine developed in this analysis is based on the PBPK model published by Robinson et al. [3] in 1992. This PBPK model accurately describes the disposition kinetics of nicotine and its major metabolite cotinine in humans. Robinson et al. derived different rates and parameters from previously published human and animal data. Then, the PBPK model was tested comparing simulations of published studies, using similar dosing protocols to those reported. Total plasma clearances [$CL_T = \text{hepatic clearance (CL}_H) + \text{renal clearance (CL}_R)$] and apparent volumes of distribution (V_d) for nicotine and cotinine were then calculated from the PBPK output.

Due to the nature of the study design presented here, those model pharmacokinetic parameters were not directly estimable and were therefore fixed to the values reported by Robinson et al [3]: (1) total plasma clearance CL_T was

fixed to 1.56 L/min for nicotine and 0.067 L/min for cotinine; (2) nicotine hepatic clearance CL_H was fixed to 1.09 L/min, where 80 % is transformed to cotinine (formation rate for cotinine [CL_{2COT}] = 0.872 L/min) [19] and the rest to other metabolites (formation rate for other metabolites [CL_{2METO}] = 0.218 L/min); (3) CL_T for cotinine (CL_{COT}) was fixed to $CL_{COT} = 0.065$ L/min ($CL_H = 0.055$ L/min and $CL_R = 0.010$ L/min); (4) V_d values for nicotine and cotinine were fixed to 207 and 73 L, respectively, based on the values reported by Robinson et al. [3]. All physiological parameters were based on population values for a 70 kg man. Both nicotine and cotinine pharmacokinetics were simultaneously described with a one-compartment linear model for each compound. Only the input parameters were estimated for this model based on the inhalation rates shown in Eq. 1.

2.4.3 Carbon Monoxide Levels: Covariate Analysis

Exhaled CO (in parts per million) is a biomarker of recent smoking history [15] that might impact the nicotine and cotinine pharmacokinetic profiles. The potential effect of this covariate was evaluated in all model parameters. As expected, a higher exhaled CO concentration was associated with higher initial concentrations for nicotine and cotinine. Linear and non-linear models were explored, connecting the initial concentrations for nicotine (NIC_0) and cotinine (COT_0) based on the CO measurements. The selected models are shown in Eq. 2 for nicotine and in Eq. 3 for its major metabolite:

$$NIC_0 = \theta_{NIC} \times (1 + CO)^{\gamma_{NIC}} \quad (2)$$

$$COT_0 = \theta_{COT} \times (1 + CO)^{\gamma_{COT}} \quad (3)$$

where CO is the individual level of carbon monoxide, θ_{NIC} and θ_{COT} are the initial concentrations for nicotine and cotinine, respectively, in the absence of CO, and γ_{NIC} and γ_{COT} are the non-linear factors.

2.4.4 Model Selection Criteria and Evaluation

The minimum objective function value (OFV) provided by NONMEM[®], which corresponds approximately to $-2 \times \log(\text{likelihood})$ [$-2LL$], served as a criteria for model comparison during the model development process. A decrease in $-2LL$ of 6.63 points for one additional parameter was regarded as a significant model improvement corresponding to a p value of 0.01 for nested models. The Akaike information criteria (AIC), calculated as $AIC = -2LL + 2 \times NP$, where NP is the number of parameters in the model, was used for selection among non-nested models [20]. The choice of the final model was based also on the OFV, the precision of parameter

estimates, goodness-of-fit plots, and individual visual predictive checks (IVPCs). Precision of parameter estimates, expressed as the 5th and 95th percentiles of the parameter distribution, were computed from the analysis of 300 bootstrap datasets (sampling with replacement). The bootstrap analysis was performed using Perl-speaks-NONMEM (PsN) [21]. Model parameter estimates were presented together (Table 1) with the corresponding relative standard error (RSE; %) as a measure of parameter imprecision computed from the results of the bootstrap analysis. The degree of ISV was expressed as a coefficient of variation (CV; %). Inspection of goodness-of-fit plots included conditional weighted residuals (CWRES) and normalized prediction distribution errors (NPDE) [22, 23]. Model performance was evaluated with IVPCs: for every subject, based on the airflow and specific individual measurements (e.g., weight and level of CO), 200 virtual individuals were simulated. At each timepoint the 2.5th, 50th, and 97.5th percentiles were calculated in every simulated study for nicotine and cotinine concentrations. Then, the 95 % prediction interval from the resultant percentiles was computed and represented over time together with the raw individual data. Predictive checks were performed using a MATLAB® environment (The MathWorks, Inc., Natick, MA, USA).

3 Results

A customized electronic nicotine delivery system, ‘custom e-cigarette’, compatible with MRI was developed (Fig. 1). The airflow recordings were used in order to establish the nicotine dose events (Fig. 2) (for one individual example, see Electronic Supplementary Material Online Resource 2). Prior to the model development, the data were explored in an attempt to evaluate the link between those recordings and the nicotine plasma concentrations. The visualization of the individual airflow patterns (Fig. 3a) and the corresponding individual pharmacokinetic profiles of the parent compound (nicotine) (Fig. 3b) indicated that the ‘custom e-cigarette’ actually delivers nicotine. Individuals with a higher number (and intensity) of dose events (inhalations) tend to have higher concentrations throughout the 90 min duration of the study.

The structure of the selected model is shown in Fig. 4; the meaning of the model parameters are shown in the legend. The corresponding NONMEM® control stream for the selected model is shown in the Electronic Supplementary Material (Online Resource 3). ISV was found to be significant for the dose scaling factor F , the distribution volume in the central compartments for cotinine (V_M), and in NIC_0 and COT_0 (Table 1). η -Shrinkage (%) was 1.14

Table 1 Pharmacokinetic parameters

Parameters	Bootstrap analysis			
	Median [2.5–97.5th percentiles]			
	Estimate (RSE %)	ISV (RSE %)	Estimate	ISV
F (min/mL·mg)	0.123 (26.87)	80.62 (49.78)	0.128 [0.087–0.196]	76.35 [18.34–104.9]
V_C (L)	207 fixed			
V_M (L)	73 fixed	30.98 (43.44)		29.34 [1.761–38.69]
CL_{2COT} (L/min)	0.872 fixed			
$CL = CL_{EX} + CL_{2METO}$ (L/min)	$CL_{2METO} = 0.218$ fixed $CL_{EX} = 0.17$ fixed			
CL_{COT} (L/min)	0.065 fixed			
θ_{NIC} (ng/mL)	7.87 (70.75)	132 (68.34)	6.475 [0.355–17.813]	117.2 [73.74–186.9]
θ_{COT} (ng/mL)	329 (39.21)	40 (45.47)	297.5 [115.3–524.0]	34.03 [12.01–48.53]
γ_{NIC} (no units)	1.5 (40.05)		1.648 [1.105–2.996]	
γ_{COT} (no units)	1.32 (18.25)		1.364 [1.059–1.789]	
$COV(\sigma_{NIC_0}, \sigma_{COT_0})$	0.527 (42.58)		0.394 [0.087–0.771]	
Residual error nicotine [$\log(\text{ng/mL})$] ^a	0.507 (14.62)		0.489 [0.378–0.611]	
Residual error cotinine [$\log(\text{ng/mL})$] ^a	0.217 (13.91)		0.210 [0.161–0.254]	

θ_{NIC} and θ_{COT} initial concentrations for nicotine and cotinine, respectively, in absence of carbon monoxide, γ_{NIC} and γ_{COT} non-linear factors, CL clearance, CL_{2COT} and CL_{2METO} formation rates for cotinine and other metabolites, respectively, CL_{EX} and CL_{COT} elimination rates for nicotine and cotinine, respectively, F scaling factor for dose calculation and bioavailability, ISV inter-subject variability, RSE relative standard error, V_C and V_M volumes of distribution of the central compartment for nicotine and cotinine, respectively

^a Additive error model in log scale

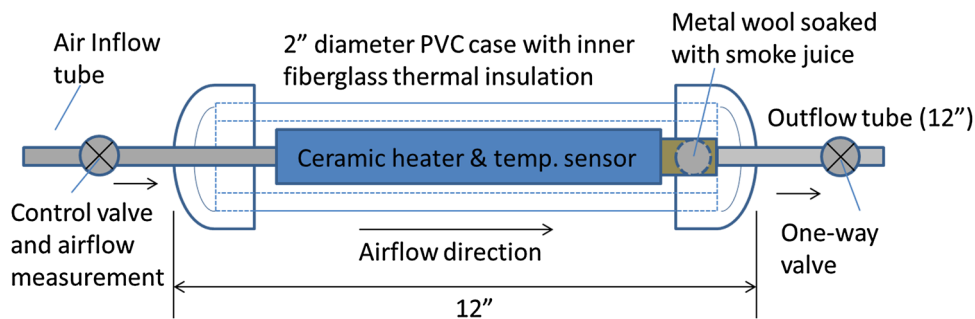


Fig. 1 Diagram of custom electronic cigarette (e-cigarette) apparatus. Air passed through a ceramic heater encased in 2-inch diameter PVC pipe, where it was heated to a controlled temperature of 300 °F. The heated air passed through a small orifice and over a 0.5-inch diameter ball of non-ferromagnetic metallic wool, which was

saturated with 0.45 mL of JC Original™ Smoke Juice (Johnson Creek Enterprises, LLC; nominal 18 mg/mL nicotine). The resulting heated vapor passed through a one-way check valve along a 12-inch section of flexible tubing and into the user's mouth. Inhaled airflow was measured in mL/min

(F), 6.55 (V_M), 3.87 (NIC_0), and 4.03 (COT_0). The inclusion of a positive correlation between the ISVs associated to the initial nicotine and cotinine concentrations [$COV(\sigma_{NIC_0}, \sigma_{COT_0})$], significantly improved the OFV provided by NONMEM, as well as the visual model fitting. Part of the variability associated with these two parameters was explained by the measured levels of CO at the beginning of the experiment. This reinforces the CO measurement as a very informative biomarker of recent smoking history. The weight of the individuals was also evaluated for correlation with the pharmacokinetic parameters but did not improve the model predictions. No other covariates were explored. Model parameter estimates are presented in Table 1 with the corresponding RSE%.

Individual and population model predictions as well as the empirical data are shown in Fig. 5. Figure 6 displays the goodness-of-fit plots for nicotine and cotinine, indicating that the selected model reasonably describes the observations. Observations were compared with the population model predictions (Fig. 6, left) as well as with individual predictions (Fig. 6, center). No dose bias and misspecifications were observed. Evaluation of the NPDE also did not show any tendency or model misspecification (Fig. 6, right).

Model performance was also evaluated with IVPCs (Fig. 7); based on the individual airflow time series, and on the corresponding individual CO levels, the 95 % predicted interval was calculated for nicotine and cotinine plasma concentrations.

4 Discussion

4.1 Efficacy

Our results demonstrate that electronic cigarettes provide effective and measurable nicotine delivery, and that the

subsequent nicotine pharmacokinetics and metabolism can be accounted for by existing models. Furthermore, with a sufficiently strong nicotine concentration in the liquid 'smoke juice' loaded into the e-cigarette, the plasma nicotine reaches lower but still comparable concentrations with those resulting from conventional cigarette smoking (Fig. 3). This demonstration of effective nicotine delivery by e-cigarettes stands in contrast with earlier reports [13, 14], but is consistent with more recent reports showing effectiveness at increasing plasma nicotine [8, 9] and also with other reports showing increased plasma cotinine as a result of e-cigarette use [10, 11]. The present results are also consistent with self-reported effectiveness at reducing nicotine cravings [4, 5].

4.2 Accuracy

Besides demonstrating the efficacy of e-cigarettes in terms of delivering nicotine, the model developed in this paper provides the first description of the concentration–time profiles for nicotine and cotinine after inhalation from an e-cigarette device. Thus, the model allows the plasma nicotine and cotinine concentrations to be predicted non-invasively. Furthermore, the developed model had well-determined parameters as evidenced by the low RSE values and predicted individual concentration profiles well. The results are consistent with earlier modeling approaches to nicotine from cigarettes [3]. Nevertheless, the results should be replicated independently in order to increase confidence in the model.

A key technical aspect of being able to manage the 5 Hz measurement frequency for the airflow was to filter what were apparent 'noise' signals that represented most of the measurements over time. It was not likely that these very low flow rates (<0.4 mL/min) would have contributed to the overall observed concentration and their inclusion would have made the modeling approach untenable. By

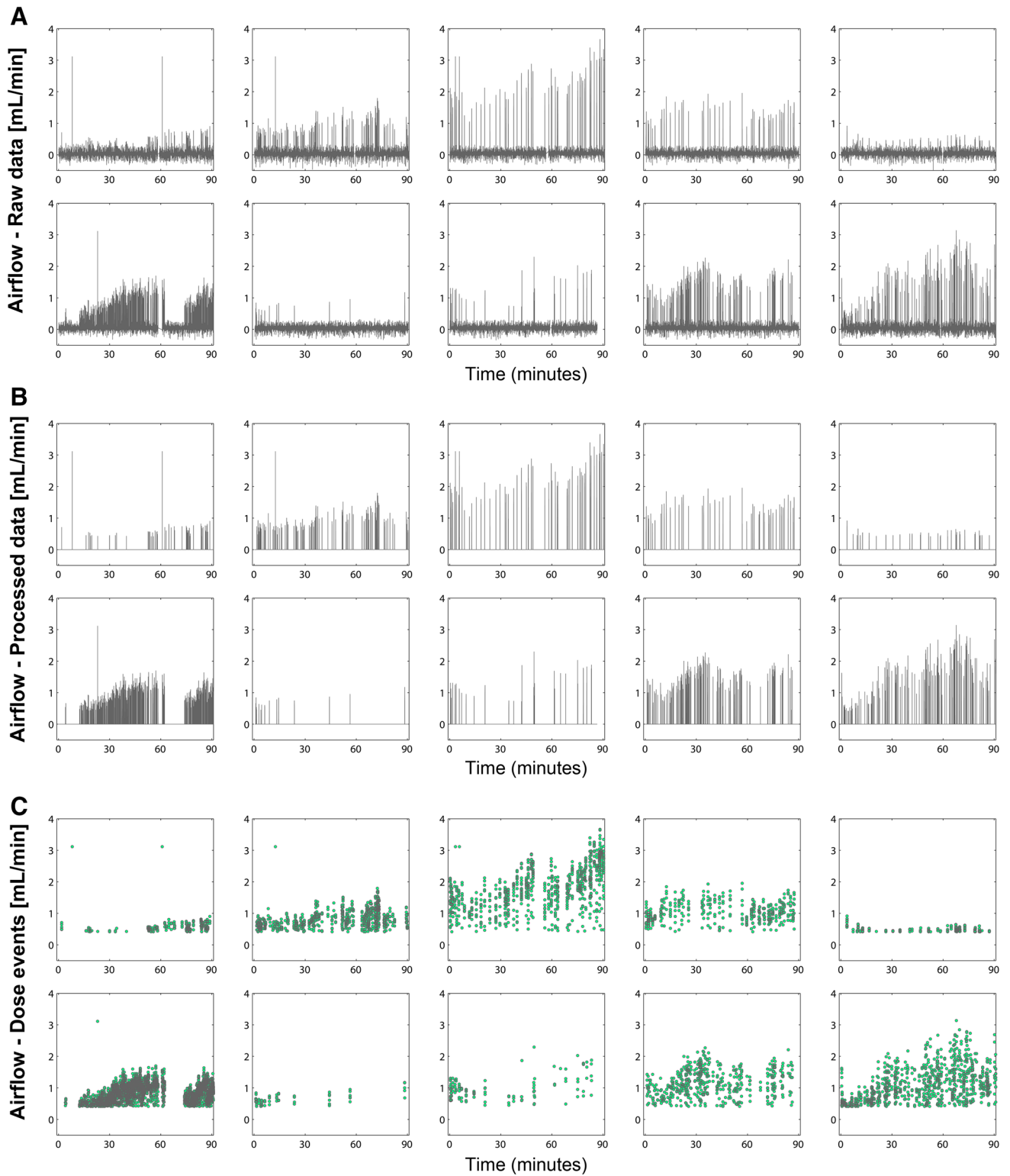


Fig. 2 **a** Airflow: raw data. **b** Airflow: processed data. The processing was developed in three consecutive steps: (1) every negative value was transformed to zero; (2) the 97.5th percentile was calculated based on all subjects; (3) every value below the 97.5th percentile was

transformed to zero. **c** Airflow: dose events. The dose events and their intensities were defined as processed airflow recordings bigger than zero (see Sect. 2 for more details)

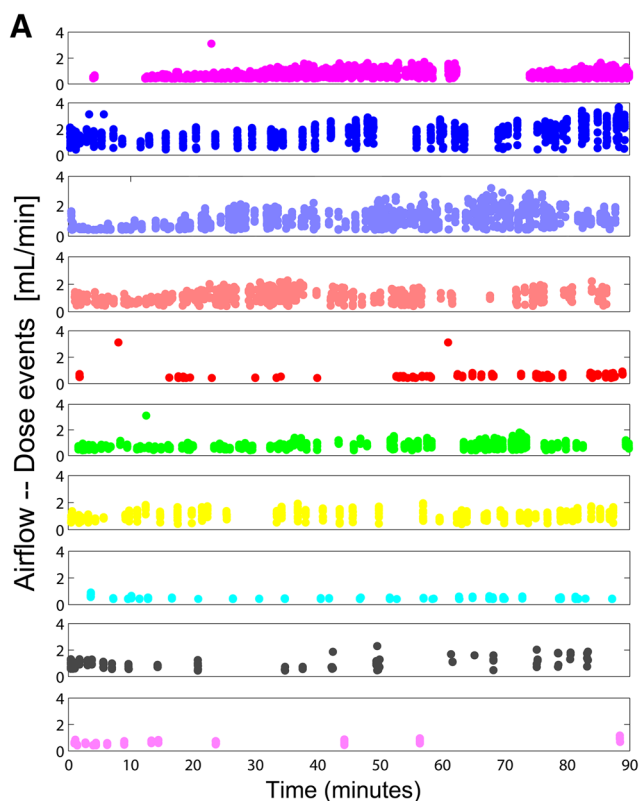
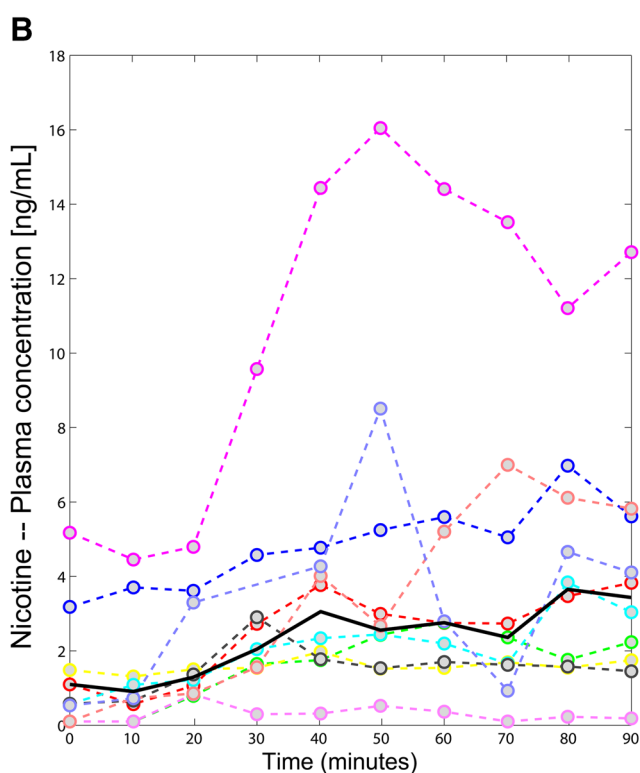


Fig. 3 a Individual dose events identified from the airflow. Every subplot corresponds to a different individual. Circles represent the dose events, which the individual is inhaling, based on the airflow measurements. **b** Individual nicotine plasma concentrations. Circles are the observed nicotine concentrations for every individual. Dashed lines are a linear interpolation between the observations. The solid



black line shows the observed median pharmacokinetics for nicotine. Every color corresponds to a different individual. The same color code was used for the individual dose events subplots, allowing the connection between airflow—dose events and the nicotine pharmacokinetic profiles

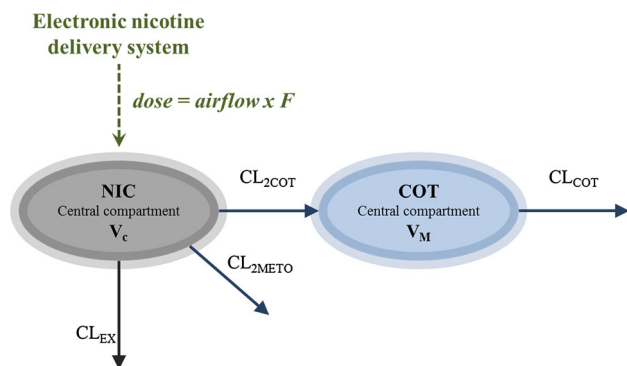


Fig. 4 Structural pharmacokinetic model for nicotine and its major metabolite cotinine. Circles represent the central compartments for nicotine and cotinine. Pharmacokinetic parameters: F scaling factor for dose calculation and bioavailability, V_C and V_M volumes of distribution of the central compartment for nicotine and cotinine, respectively, CL_{2COT} and CL_{2METO} formation rates for cotinine and other metabolites respectively, CL_{EX} and CL_{COT} elimination rates for nicotine and cotinine, respectively. *COT* cotinine, *NIC* nicotine

filtering above the 97.5th percentile, key input events for nicotine inhalation/dose delivery were captured (see Fig. 1b, c).

The accuracy of the model depends on having a good estimate of the initial conditions of plasma concentrations. We explicitly measured the starting plasma concentrations, and we additionally measured exhaled CO as an additional (though limited) correlate of initial plasma concentrations. The exhaled CO is only useful as a predictor of recent cigarette smoking and would not be expected to correlate with recent e-cigarette usage, as these generate no significant CO. The CO is primarily utilized to predict the baseline concentrations and, at least statistically, significantly improved the description by the model of the baseline values. Thus, it is not the CO that is the target of interest but rather the impact on predicting the likely baseline nicotine concentration where this CO measure appears to be useful. Still, if e-cigarette airflow is measured for a sufficiently long period of time, the impact of the initial conditions (and associated inaccuracies) will diminish toward zero over time.

4.3 E-Cigarettes

Many questions remain unanswered regarding the safety and effectiveness of e-cigarettes, especially as aids to

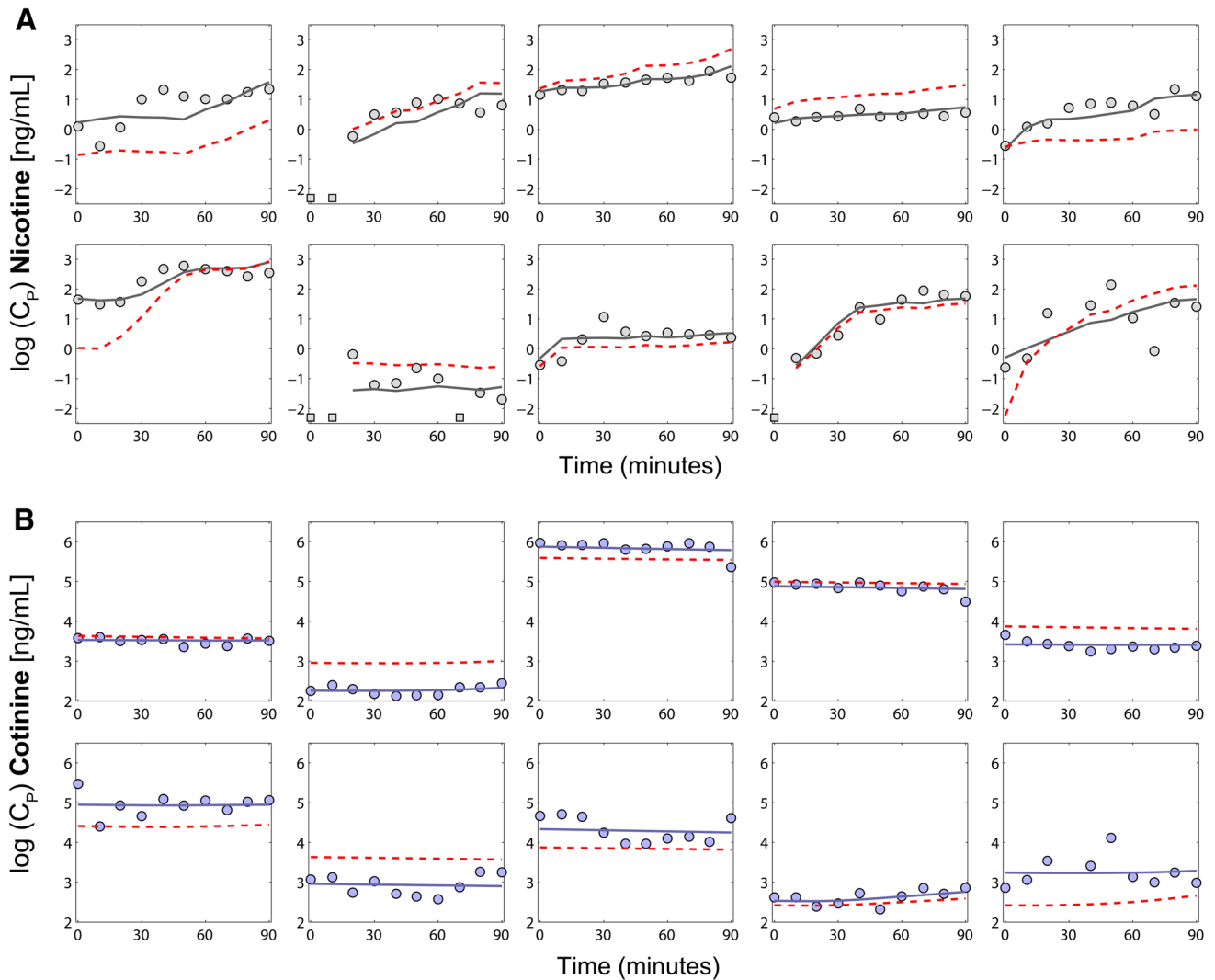


Fig. 5 Individual predictions versus observations for nicotine (a) and cotinine (b). The gray colors in a denote nicotine, and the light blue colors in b denote cotinine. Circles represent observations above the minimum quantification level. Squares represent observations below

the quantification level. The red dashed lines represent the population prediction. The solid lines represent the individual predictions. C_p plasma concentration

smoking cessation. Our results do not address whether e-cigarettes are safe for the public, although our very modest sample size revealed no immediate adverse events. Our results also do not indicate whether e-cigarettes are effective as an aid to smoking cessation. What our results do show as a first step, however, is that e-cigarettes can be effective in delivering nicotine specifically in a way that is well-characterized by our pharmacokinetic model.

As e-cigarette use becomes more and more common, understanding associated nicotine delivery and both cognitive and addictive effects will become more important. This model represents a tool that can help to more precisely understand the relationship between the inhalation delivered nicotine dose and nicotine and cotinine plasma concentrations. The plasma concentrations can then be

evaluated in the context of any number of target responses or toxicities.

Looking ahead, we are currently planning to use our custom e-cigarette device to carry out functional neuroimaging studies of e-cigarette use. The present study provides a foundation for our planned functional neuroimaging, as our device is MRI-compatible. In this way, it will be possible to predict plasma nicotine and cotinine concentrations in subjects without having to simultaneously draw blood. This non-invasive approach may be particularly helpful in experiments involving many interventions, where the action of a blood draw may skew patient responses in MRI-based studies as well as increase the costs associated with the study. This first issue is particularly important when assessing the cognitive and

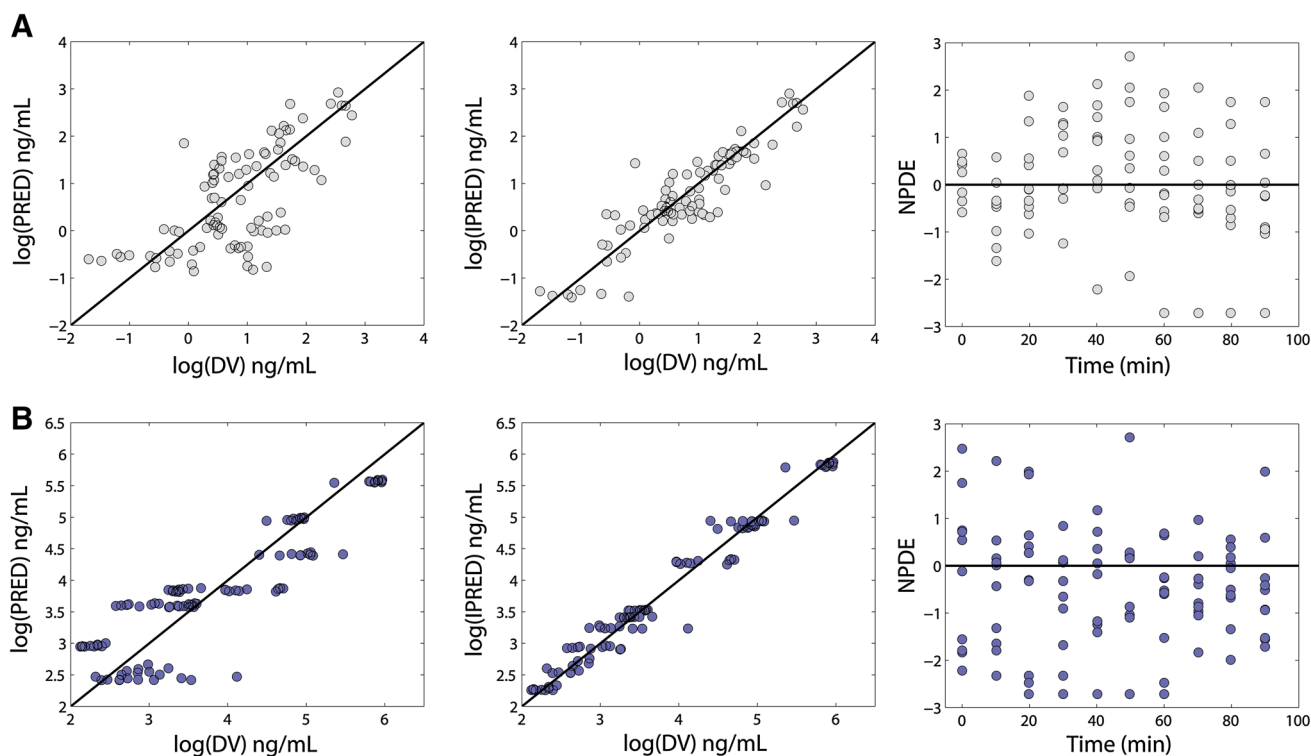


Fig. 6 Goodness-of-fit plots of the selected population pharmacokinetic model for **a** nicotine (gray) and **b** cotinine (light blue). Solid lines show the identity lines for the first two columns and the zero line

for the last column. *DV* dependent variable, *IPRED* individual model predictions, *NPDE* normalized prediction distribution errors, *PRED* population model predictions

addiction liability effects of nicotine inhalation using the MRI paradigm.

4.4 Limitations

The study has several limitations. Our custom e-cigarette was designed to be MRI-compatible and, as such, it may not be identical to e-cigarettes available on the open market. We did not directly compare our custom e-cigarette against commercial e-cigarettes. The commercial e-cigarettes may vary among brands in their effectiveness at delivering nicotine. Likewise, available smoke juice formulations may differ in composition and effective bioavailability. Thus, we have not shown that every available e-cigarette effectively delivers nicotine, and it is beyond the scope of the current study to do so. Also, we have not shown that every available e-cigarette smoke juice effectively delivers nicotine, as the effective bioavailability may vary as a function of solution pH and other ingredients in the smoke juice. The estimated value for the scaling factor F will have to be re-estimated if other e-cigarettes are used, since it could vary among brands. Due to the data available and study design, other factors that might affect nicotine delivery have not been explored here.

Our study specifically showed that at least the present custom e-cigarette with an airflow temperature of 300 °F

over a non-combustible medium (metallic wool) and with the particular smoke juice can effectively deliver nicotine. Also, we have shown that the nicotine delivery can be accounted for with a pharmacokinetic model similar to one that is valid for regular cigarettes, as a function of inhaled e-cigarette vapor volume. Another potential limitation of the current study is that e-cigarette users become more proficient at using the e-cigarette over time, so that they are able to increase their plasma nicotine concentrations more effectively after a few weeks of use. We did not control for the length of time subjects had used e-cigarettes. However, our recruitment criteria required that subjects be current heavy smokers with no stated intention of quitting. This means that our subjects were generally not e-cigarette users, and they would therefore be less proficient at increasing their plasma nicotine concentrations. The fact that we found measurable plasma nicotine increases suggests that the relative lack of experience did not prevent them from obtaining nicotine from our custom e-cigarette. Furthermore, our detailed measurements of airflow account for any individual differences based on levels of experience with e-cigarettes. Finally, due to the limited sample size of the present study, the model we present here should be validated in an independent sample of subjects.

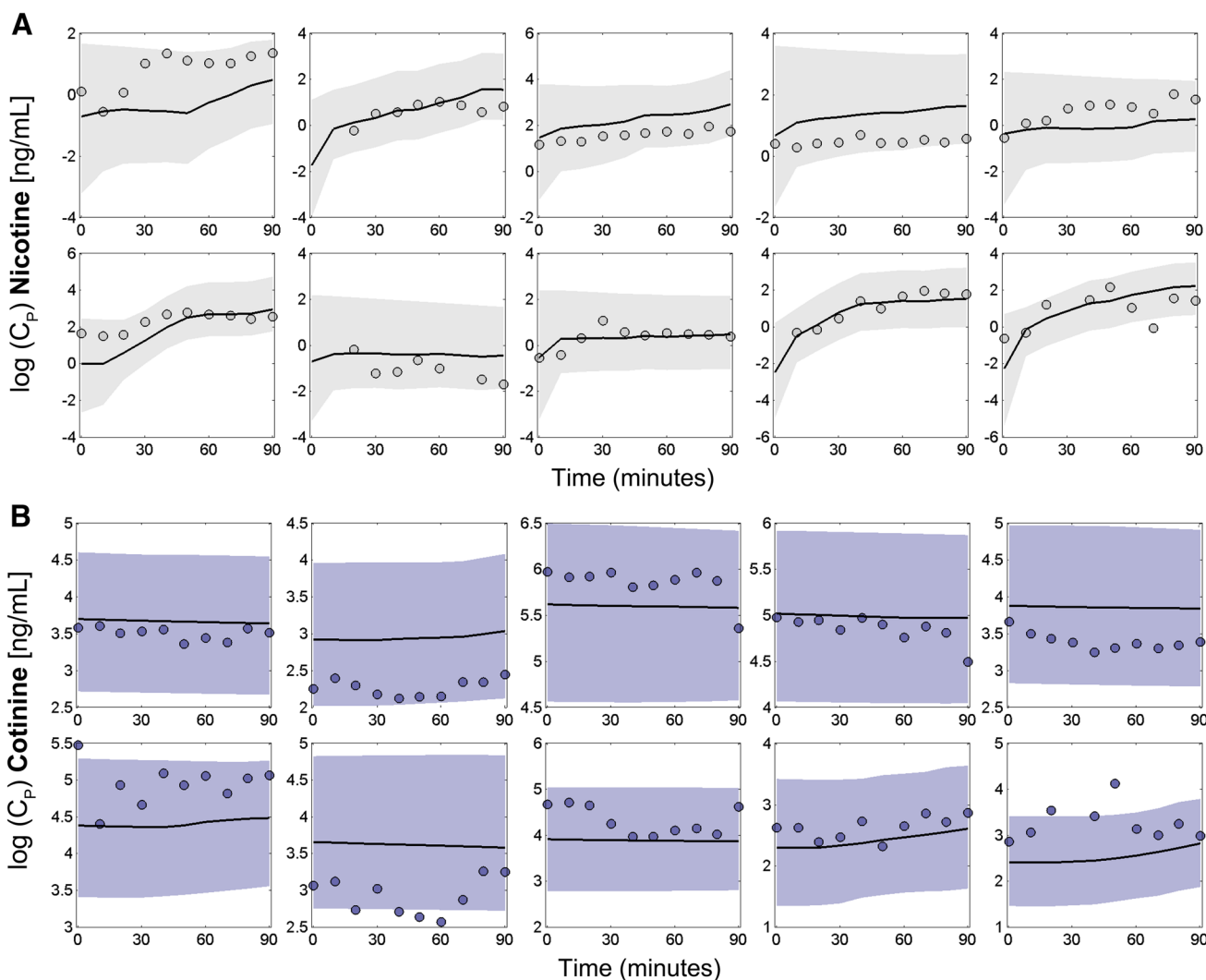


Fig. 7 Individual visual predictive checks: results from 200 simulated studies. *Shaded areas* represent the 95 % prediction interval for every individual based on their airflow, carbon monoxide levels and weight. The *black lines* correspond to the median of the simulated

subjects. *Points* are the observations. The *gray color* stands for nicotine (a) and *light blue* for the major metabolite cotinine (b). C_p plasma concentration

5 Conclusion

We developed a well-estimated population pharmacokinetic model for plasma concentrations of nicotine and cotinine after e-cigarette nicotine delivery and this will provide the basis for the determination of typical nicotine concentrations for any given pattern of e-cigarette-associated airflow delivery of nicotine.

Acknowledgments We thank the Disease and Therapeutic Response Modeling Program for the Clinical and Translational Sciences Institute (CTSI) at Indiana University. We thank Karmen Dayhuff and Andrea Meyer for assistance with blood draws, Jeff Sturgeon for designing and implementing the custom electronic cigarette, and Ken Mackie for providing facilities to process the blood plasma. Supported by the Indiana Clinical Translational Sciences Institute, CPAC Core facility grant (JWB, DRJ). Supported by the Indiana Clinical and Translational Sciences Institute, funded in part

by grant # RR 02576 from the National Institutes of Health, National Center for Research Resources. Analytical work was performed by the Clinical Pharmacology Analytical Core laboratory, a core laboratory of the Indiana University Melvin and Bren Simon Cancer Center supported by the National Cancer Institute grant P30 CA082709. NVM was supported by Eli Lilly and Company through the Indiana Clinical and Translational Sciences Institute (CTSI).

References

1. Yamazaki H, Horiuchi K, Takano R, Nagano T, Shimizu M, Kitajima M, et al. Human blood concentrations of cotinine, a biomonitoring marker for tobacco smoke, extrapolated from nicotine metabolism in rats and humans and physiologically based pharmacokinetic modeling. *Int J Environ Res Public Health*. 2010;7:3406–21.
2. Teeguarden JG, Housand CJ, Smith JN, Hinderliter PM, Gunawan R, Timchalk CA. A multi-route model of nicotine–cotinine

- pharmacokinetics, pharmacodynamics and brain nicotinic acetylcholine receptor binding in humans. *Regul Toxicol Pharmacol*. 2013;65:12–28.
3. Robinson DE, Balter NJ, Schwartz SL. A physiologically based pharmacokinetic model for nicotine and cotinine in man. *J Pharmacokinet Biopharm*. 1992;20:591–609.
 4. Etter JF, Bullen C. Electronic cigarette: users profile, utilization, satisfaction and perceived efficacy. *Addiction*. 2011;106:2017–28.
 5. Caponnetto P, Campagna D, Cibella F, Morjaria JB, Caruso M, Russo C, et al. Efficiency and Safety of an eLectronic cigAreTte (ECLAT) as tobacco cigarettes substitute: a prospective 12-month randomized control design study. *PLoS One*. 2013;8:e66317.
 6. Cheng T. Chemical evaluation of electronic cigarettes. *Tob Control*. 2014;23(Suppl 2):ii11–7.
 7. Grana R, Benowitz N, Glantz SA. E-cigarettes: a scientific review. *Circulation*. 2014;129:1972–86.
 8. Dawkins L, Corcoran O. Acute electronic cigarette use: nicotine delivery and subjective effects in regular users. *Psychopharmacology (Berl)*. 2014;231:401–7.
 9. Vansickel AR, Eissenberg T. Electronic cigarettes: effective nicotine delivery after acute administration. *Nicotine Tob Res*. 2013;15:267–70.
 10. Flouris AD, Poulianiti KP, Chorti MS, Jamurtas AZ, Kouretas D, Owolabi EO, et al. Acute effects of electronic and tobacco cigarette smoking on complete blood count. *Food Chem Toxicol*. 2012;50:3600–3.
 11. Schroeder MJ, Hoffman AC. Electronic cigarettes and nicotine clinical pharmacology. *Tob Control*. 2014;23(Suppl 2):ii30–5.
 12. Hajek P, Goniewicz ML, Phillips A, Myers SK, West O, McRobbie H. Nicotine intake from electronic cigarettes on initial use and after 4 weeks of regular use. *Nicotine Tob Res*. Epub 2014 Aug 13.
 13. Vansickel AR, Cobb CO, Weaver MF, Eissenberg TE. A clinical laboratory model for evaluating the acute effects of electronic “cigarettes”: nicotine delivery profile and cardiovascular and subjective effects. *Cancer Epidemiol Biomarkers Prev*. 2010;19:1945–53.
 14. Eissenberg T. Electronic nicotine delivery devices: ineffective nicotine delivery and craving suppression after acute administration. *Tob Control*. 2010;19:87–8.
 15. Middleton ET, Morice AH. Breath carbon monoxide as an indication of smoking habit. *Chest*. 2000;117:758–63.
 16. Hukkanen J, Jacob P III, Benowitz NL. Metabolism and disposition kinetics of nicotine. *Pharmacol Rev*. 2005;57:79–115.
 17. Armitage AK, Dollery CT, George CF, Houseman TH, Lewis PJ, Turner DM. Absorption and metabolism of nicotine from cigarettes. *Br Med J*. 1975;4:313–6.
 18. Beal SL. Ways to fit a PK model with some data below the quantification limit. *J Pharmacokinet Pharmacodyn*. 2001;28:481–504.
 19. Benowitz NL, Porchet H, Jacob P III. Nicotine dependence and tolerance in man: pharmacokinetic and pharmacodynamic investigations. *Prog Brain Res*. 1989;79:279–87.
 20. Ludden TM, Beal SL, Sheiner LB. Comparison of the Akaike Information Criterion, the Schwarz criterion and the *F* test as guides to model selection. *J Pharmacokinet Biopharm*. 1994;22:431–45.
 21. Lindbom L, Ribbing J, Jonsson EN. Perl-speaks-NONMEM (PsN)—a Perl module for NONMEM related programming. *Comput Methods Programs Biomed*. 2004;75:85–94.
 22. Hooker AC, Staats CE, Karlsson MO. Conditional weighted residuals (CWRES): a model diagnostic for the FOCE method. *Pharm Res*. 2007;24:2187–97.
 23. Comets E, Brendel K, Mentre F. Computing normalised prediction distribution errors to evaluate nonlinear mixed-effect models: the npde add-on package for R. *Comput Methods Programs Biomed*. 2008;90:154–66.